Evidence and mechanisms of selenate reduction to extracellular elemental selenium nanoparticles on the biocathode

Zhiming Zhang[a,†], Benhur K. Asefaw[a,†], Yi Xiong[a], Huan Chen[b], Youneng Tang[a,*]

[a] Department of Civil and Environmental Engineering, FAMU-FSU College of Engineering, Florida State University, 2525 Pottsdamer Street, Tallahassee, Florida 32310, United States

[b] National High Magnetic Field Laboratory, Florida State University, 1800 East Paul Dirac Drive, Tallahassee, Florida 32310, United States

†The two authors equally contributed to this work.

*Phone: +1(850)410-6119; e-mail: ytang@eng.famu.fsu.edu

ABSTRACT

Intracellular selenium nanoparticles (SeNPs) production is a roadblock to the recovery of selenium from biological water treatment processes because it is energy-intensive to break microbial cells and then separate SeNPs. This study provided evidence of significantly more extracellular SeNPs production on the biocathode (97-99%) compared to the conventional reactors (1-90%) using transmission electron microscopy coupled with energy-dispersive X-ray spectroscopy. The cathodic microbial community analysis showed that relative abundance of *Azospira oryzae*, *Desulfovibrio*, *Stenotrophomonas*, and *Rhodocyclaceae* were < 1% in the inoculum but enriched to 10% - 21% for each group when the bioelectrochemical reactor reached a steady state. These four groups of microorganisms simultaneously produce intracellular and extracellular SeNPs in conventional biofilm reactors per literature review but prefer to produce extracellular SeNPs on the cathode. This observation may be explained by the cellular energetics: By producing extracellular SeNPs on the biocathode, microbes do not need to transfer selenate and the electrons from the cathode into the cells, thereby saving energy. Extracellular SeNPs production on the biocathode is feasible since we found high concentrations of C-type cytochrome, which is well known for its ability to transfer electrons from electrodes to microbial cells and reduce selenate to SeNPs on the cell membrane.

KEYWORDS: Biocathode, selenate, extracellular selenium nanoparticles, transmission electron microscope

SYNOPSIS: This work presents a novel method for recovering selenium, a high-risk element vulnerable to supply and other restrictions.

36 **Table of Contents**

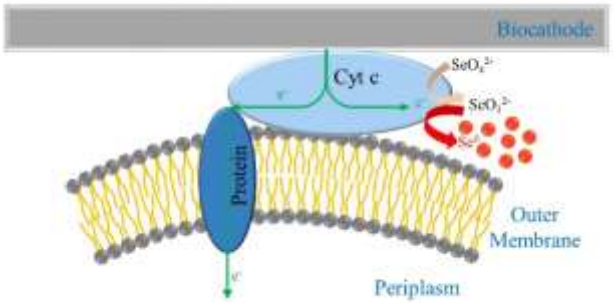

37

1. INTRODUCTION

Selenium (Se) is a naturally occurring trace element in Earth's crust. It is a micronutrient for humans and wildlife but toxic at high concentrations. U.S. Environmental Protection Agency has established a maximum contaminant level of 50 μg Se/L of total selenium in drinking.[1] Among all the selenium species in contaminated surface water, selenate (SeO_4^{2-}) is predominant in most settings.[2] Various physical and chemical approaches such as reverse osmosis and ion exchange are utilized to separate selenate from water.[3] Biological selenate removal has been widely studied in the recent three decades due to its ability to convert selenate and its potentially low costs.[4–7] Microbes convert selenate to elemental selenium nanoparticles (SeNPs), which can be further separated from water.[8]

In recent years, many researchers attempted to recover SeNPs that were produced in biological reactors.[9,10] Recovery of SeNPs not only prevents secondary contamination of the residues (e.g., via disposal of sludge that contains SeNPs in high concentrations), but also offsets the treatment costs since selenium is widely used in various industrial applications such as semiconductors and alloys.[5,11] Selenium is one of the 23 mineral commodities viewed as important to the national economy and national security of the United States,[12] one of the critical elements for low carbon energy technologies,[13,14] and one of the high-risk elements vulnerable to supply and other restrictions.[14,15] One roadblock to SeNPs recovery is that conventional biological reactors reduce selenate to mainly intracellular SeNPs.[16] While extracellular SeNPs may be separated from biomass for recovery via centrifugation[17] or selective adsorption[6], the intracellular SeNPs are much more difficult to separate and recover since an additional cell lysis step is required. Although cell

lysis can be achieved using lysozyme and French press, liquid nitrogen, and sonication,[18,19] the processes are energy-intensive and require chemical addition.

In our previous work, we used a biocathode-based bioelectrochemical reactor (BEC_1) to remove selenate and found that the reactor produced mainly extracellular spherical nanoparticles (likely SeNPs), while the selenate reduction was negligible in two control reactors (*i.e.*, sterile cathode control and open circuit mode control).[16] The BEC_1 reactor was inoculated with a combination of activated sludge from a local municipal wastewater treatment plant and leachate from a local landfill. Regardless of the inoculum, confirming the biocathode's ability of producing mainly extracellular spherical nanoparticles is of interest. Hence, the first objective of the current work is comparison with conventional reactors for production of extracellular selenium nanoparticles. This includes direct comparison through our experiments and indirect comparison through literature review. The second objective is to demonstrate that different biomass seeds lead to similar results. This is very important because one could argue that since we only used one biomass seed in our previous publication, the extracellular selenium nanoparticles production could be a coincidence if that biomass seed happened to contain little intracellular-selenium-producing bacteria. In this report, we quantify bacteria that produce intracellular versus extracellular selenium nanoparticles.

Through thin-section transmission electron microscopy (TEM) analysis in our previous work [16], we observed that almost all spherical and dense particles are extracellular, thereby seeing the potential of biocathode for producing mainly extracellular SeNPs. The third objective of the current work is to provide direct evidence of mainly extracellular SeNPs production on the

biocathode through morphology analysis by TEM combined with elemental analysis by energy-dispersive X-ray spectroscopy (EDX), and through comparing to a conventional reactor control. The fourth objective is to gain insights into the mechanisms of extracellular SeNPs production on the biocathode by analyzing the microbial community change and a key enzyme involved in SeNPs production. The last objective is to further determine the mechanisms based on cellular energetics.

2. MATERIALS AND METHODS

2.1 Reactors Operation

Two BEC reactors (BEC_2 and BEC_3) shown in Figure S1 and one conventional reactor as a control were operated in the current study. BEC_2 was the same as the BEC_1 in our previous work [16], but the inoculum for the anodic and cathodic chambers was changed to activated sludge from a local municipal wastewater treatment facility. While reactor details can be found in Zhang et al.[16], BEC_2 is briefly summarized as follows. Two plain carbon electrodes (*i.e.*, the anode and biocathode, 2.5 cm × 6 cm, Fuel Cell Store, USA) were immersed in the activated sludge sample for 12 days and then transferred into the two chambers of the BEC_2 reactor, respectively. The anode and biocathode were externally connected to a resistor (100 Ω). After introducing the electrodes, the anodic chamber was continuously fed with a deoxygenated mineral medium[16] amended with sodium acetate (CH_3COONa, 10 mg C/L) as the electron donor[16]. The cathodic chamber was fed with the same medium amended with sodium selenate (Na_2SeO_4, 5 mg Se/L) as the electron acceptor. The two chambers were separated by a cation exchange membrane (CEM, model CMI-7000, Membranes International Inc., USA). BEC_2 cathode was operated at a constant flow rate of 200 mL/day, corresponding to a hydraulic residence time of 1.45 days and a selenate surface loading rate of 330 mg Se/m^2-day. BEC_3 was the same as BEC_2, but the selenate surface loading rate was reduced to 50 mg Se/m^2-day by decreasing the flow rate to 75 mL/day and the influent selenate concentration to 2 mg Se/L. The selenate surface loading rates (50 and 330 mg Se/m^2-day) were close to the higher end of the selenate surface loading rate ranges reported for conventional biofilm reactors: 0.29 – 362 mg Se/m^2-day.[20–24] The anodic chamber of BEC_2 was operated at a constant flow rate of 200 mL/day, corresponding to an acetate loading rate of 660

mg C/m^2-day. The anodic chamber of BEC_3 was the same as BEC_2, but the flow rate was reduced to 75 mL/day, and the acetate loading rate was reduced to 250 mg C/m^2-day (Table 1).

A column packed with plastic media (BioFLO 9, Smoky Mountain Bio Media) for biofilm attachment was operated as a conventional reactor control. The operating conditions for this control and BEC_2 were the same. For instance, the selenate surface loading rate was also 330 mg Se/m^2-day. Figure S2 shows the schematics of this control reactor.

2.2 Chemical Analysis

To determine selenate reduction and its products in the BEC_2 and BEC_3 reactors, and the conventional reactor control, the influent and effluent of these reactors were sampled every three days and analyzed for selenate in the influent ($[SeO_4^{2-}]_{in}$) and various selenium species after the biological reduction, including three dissolved selenium species (selenate in the effluent, $[SeO_4^{2-}]_{eff}$; selenite in the effluent, $[SeO_3^{2-}]_{eff}$; and selenide in the effluent, $[Se^{2-}]_{eff}$), and solid selenium estimated through mass balance ($[Se]_{solid} = [SeO_4^{2-}]_{in} - [SeO_4^{2-}]_{eff} - [SeO_3^{2-}]_{eff} - [Se^{2-}]_{eff}$). The particulate selenium concentration was calculated as the difference between the total and dissolved selenium concentrations.[25] Based on the recovery tests in which known concentrations of dissolved selenium, solid selenium nanoparticles, and biomass were added to deionized water, groundwater and surface water, the recovery of the dissolved selenium after removing the particulate selenium varied between 96-104%.

To further characterize the extracellular versus intracellular nanoparticles production, TEM (Hitachi HT7800, USA) was used to analyze solid samples from the inoculum, the conventional

reactor (samples from the biofilm coated plastic media), and the BEC_2 and BEC_3 reactors (samples from both biocathodes and effluent of the cathodic chambers) when the reactors reached steady state. To confirm that the nanoparticles were SeNPs, annular dark-field Scanning Transmission Electron Microscopy (ADF-STEM, JEM-ARM200cF, USA) with EDX was further used for selected solid samples, including samples from the biocathode of BEC_2 and the conventional reactor control. To provide additional lines of evidence for the extracellular SeNPs production, the selected solid samples were also analyzed by Raman spectroscopy (Renishaw InVia Confocal Raman Microscopy, Renishaw, USA) and Scanning Electron Microscopy (SEM, FEI Nova 400 Nano SEM, FEI, USA) coupled with EDX.

Acetate in the anodic chamber of both reactors (BEC_2 and BEC_3) and the conventional reactor was measured using ion chromatography (Dionex Aquion Ion Chromatography System, USA, quantification limit 50 μg C/L). Sulfate in both chambers of BEC_2 and BEC_3 reactors and the control reactor (conventional reactor) was also measured using ion chromatography (quantification limit: 20 μg S/L).

The detailed procedure for TEM, SEM, Raman spectroscopic analysis, and the sample pretreatment are described in Supporting Information (SI). The detailed methods for the measurement of other parameters discussed in this section are available in our previous publication.[16]

155 **2.3 Electrochemical Analysis**

156 We used four parameters to evaluate the electrochemical performance of the bioelectrochemical
157 reactors. Voltage across the external resistor (100 Ω) was measured by a multimeter (MU 113,
158 Electronic Resources LTD, USA). Current was calculated by dividing the voltage by the external
159 resistance (100 Ω). Current density (mA/m^2) at steady state was calculated by dividing current by
160 the total surface area of an electrode (3×10^{-3} m^2). Coulombic efficiency was calculated by dividing
161 the electrons transferred from the anode to the cathode by the electron donor (acetate in our case)
162 consumed in the anode chamber. The detailed methods for the above analysis were described in
163 Zhang et al.[16]

164

165 **2.4 Microbial Community Analysis**

166 Because the chemical and electrochemical performance of the three BEC reactors were similar,
167 we chose the BEC_1 reactor, the first tested reactor, to analyze its microbial community. Five
168 biomass samples were taken: one sample at the beginning of the experiment from the inoculum
169 and four samples at the end of the experiment from the biocathode, the cathodic effluent, the anode,
170 and the anodic effluent, respectively. Method details for DNA extraction and 16S rRNA
171 sequencing were described in SI.

172

3. RESULTS AND DISCUSSION

3.1 Chemical and Electrochemical Performance of Reactors

The changes of selenium speciation with time for BEC_2 and BEC_3 reactors were similar and presented in detail in Figure 1. In both cathodic chambers of the BEC_2 and BEC_3 reactors, selenate (SeO_4^{2-}) started to be reduced on the third day of operation and reached below the quantification limit of 0.02 mg Se/L during steady state. Selenite (SeO_3^{2-}) accumulated first, but almost disappeared (close to the quantification limit of 0.02 mg Se/L) during the steady state. More than 90% of the selenate (SeO_4^{2-}) was reduced to particulate selenium in both reactors. Despite the different inoculum and selenate loading rates, the trends of selenium species change in BEC_2 and BEC_3 were similar to the trends for BEC_1 in our previous research.[16] The conventional reactor control was also able to reduce 97% of the influent selenate (SeO_4^{2-}) to particulate selenium. Other selenium species produced in this control reactor were below detection limits during the steady state.

Table 1 compares the steady state performance of the BEC_1 reactor[16], its sterile cathode control [16], its open circuit control [16], the BEC_2 reactor (the same as BEC_1 except for the inoculum), the BEC_3 reactor (the same as BEC_2 except for a lower selenate loading rate), and the conventional reactor. The operation of BEC_1 and BEC_2 differed only in the inoculum: a mixture of activated sludge and landfill leachate for BEC_1 and activated sludge for BEC_2. The major difference in reactor performance was that 30% more acetate was consumed in the anodic chamber of BEC_2, which likely stimulated the growth of more sulfate-reducing bacteria in the anodic chamber of BEC_2 (supported by the sulfate data in Table 1). This further led to a lower current density in BEC_2 (40 mA/m^2) compared to BEC_1 (86 mA/m^2). Nevertheless, the more growth of sulfate-reducing

196 bacteria and methanogens did not cause a significant difference in selenate reduction between
197 BEC_1 and BEC_2.

198

199 The operation of BEC_3 differed from BEC_2 in the selenate loading rate: 50 mg Se/m^2-day for
200 BEC_3 and 330 mg Se/m^2-day for BEC_2. This directly led to the lower current density in BEC_3 (22
201 mA/m^2) compared to BEC_2 (40 mA/m^2), but did not significantly affect the selenate reduction: >90%
202 of selenate in the influent were converted to particulate selenium by the reactors. The current
203 density in these reactors (22 to 86 mA/m^2) was comparable to anaerobic two-chamber biocathode
204 reactors reported in the literature for reduction of nitrate and chromium (IV): 3 to 123 mA/m^2.[26,27]

205

206 From the three control reactors tested, the cathodic chamber of both controls (sterile cathode and
207 open circuit mode) showed negligible (< 0.05 mg Se/L) reduction of selenate. This confirms that
208 the selenate reduction was dependent on the electron transfer from the anodic chamber to the
209 cathodic chamber across the external circuit and the electron transfer to bacteria on the biocathode.
210 The conventional reactor was used as a control to confirm that the BEC reactors produced
211 significantly more extracellular elemental selenium, which is further discussed in the next section.

212

213 **3.2 Intracellular Versus Extracellular Production of SeNPs**

214 Figure 2 compares representative thin-section TEM images of particulate mixtures from the
215 inoculum, BEC_2, BEC_3, and conventional biofilm reactor. Both intracellular and extracellular
216 nanoparticles that were dense and spherical were commonly found in the inoculum and the
217 conventional reactor control. However, almost all of the dense and spherical nanoparticles

associated cathodic chamber of BEC_2 and BEC_3 were extracellular. Selenate was added to the inoculum samples here to analyze the location of produced nanoparticles.

To further quantify the percentage of cells with intracellular, dense and spherical nanoparticles in the TEM images, Table 2 compares this number among various studies. The percentages of cells with intracellular nanoparticles were ~2% for BEC_2 (this study), ~3% for BEC_3 (this study), and ~1% in BEC_1 of our previous study [16]. These numbers were consistently lower than the ~25% for the conventional reactor control in this study. The comparison is based on 50 TEM images like those shown in Figure 2. They are also consistently lower than the numbers (10-99%) reported in previous studies with conventional reactors.[28–33]

In addition to the location differences of intracellular versus the extracellular dense and spherical Se particles, the reactors also differed in the size of these particles produced. The diameters of the particles were smaller in BEC_3 compared to the other reactors. This can be explained by the fact that the selenate loading rate in BEC_3 was 15% of the loading rate in the other reactors (See Table 1). SeNPs formation started with Se nucleation seeds, followed by deposition of more Se^0 onto the seeds.[34] Therefore, a higher loading rate led to more deposition of Se and larger SeNPs.

The EDX map collected in the STEM mode with a probe size of 0.12 nm confirmed that the dense spherical nanoparticles in the TEM images were elemental selenium nanoparticles. Figure 3 shows the EDX mapping spectra for two representative particulate samples taken from the biocathode of BEC_2 and the conventional reactor control, respectively. The predominant element in all dense and spherical nanoparticles of such STEM images was selenium. The SEM images and their EDX

241 analysis of particle samples taken from the cathodic chambers of BEC_2 and BEC_3 (See Figure 4)
242 also consistently show that the dense and spherical nanoparticles were elemental selenium
243 nanoparticles. Raman spectra analysis of the samples taken from the biocathode of BEC_3 further
244 showed that the elemental selenium was trigonal (237 cm^{-1}, Figure S5) and amorphous (255 cm^{-1},
245 Figure S5). No spherical nanoparticles (elemental selenium) were produced in the anodic
246 chambers, which confirmed neither selenate reduction nor diffusion from the cathode side through
247 the cation exchange membrane (Figure S3).

248

249 **3.3 Microbial Community in BEC_1**

250 The heatmap in Figure 5 shows the OTUs in five samples (the inoculum, biocathode, cathodic
251 effluent, anode, and anodic effluent) taken at steady state for BEC_1. The OTUs are representative
252 based on the rarefaction curves (Figure S4 in SI).[35] Compared to the microbial community in
253 inoculum, five major microbial groups were enriched on the biocathode, including *Azospira oryzae*
254 (21%), *Methanobacterium curvum* (19%), *Desulfovibrio* (16%), *Stenotrophomonas* (16%), and
255 *Rhodocyclaceae* (9.6%), all of which were less than 1% in the inoculum (Figure 5).

256

257 After literature review, we found that four out of the five groups (except for *Methanobacterium*
258 *curvum*) could use selenate as the electron acceptor. *Azospira oryzae*, *Desulfovibrio*, and
259 *Stenotrophomonas* are reported to produce both intracellular and extracellular SeNPs in
260 conventional reactors, where an electron donor and selenate are mixed in the liquid (Table S1).
261 Many species such as *Azoarcus sp.* and *Zooglea ramigera*, in the family of *Rhodocyclaceae*, are
262 reported to produce intracellular and extracellular SeNPs (Table S1). Interestingly, the four
263 microbial groups almost exclusively produced extracellular SeNPs (99%, see Table 2) by using

electrons from the biocathode. The electrons for microbes to reduce selenate in the cathodic chamber must be from the biocathode because there was no selenate reduction in the sterile cathode control and the open circuit control (See Table 1). The sterile cathode control demonstrated that the selenate was reduced by microbes in the biocathode chamber. The open circuit control further demonstrated that the electrons for microbial selenate reduction was from the biocathode.

All the top four abundant groups of selenate-reducing microorganisms on the biocathode (See Table S1) are rod-shaped.[36–38] This morphology is consistent with all the SEM images (Figure S3 and Figure 4). While the TEM cell images in Figure 2 show both rod and round shapes, both could represent rod-shaped microorganisms since the TEM images only show thin sections of the microorganisms.[39]

Among the top five abundant groups of microorganisms on the biocathode (See Table S1), three groups could potentially accept electrons from the biocathode, considering that electron transfer mechanisms on the biocathode are similar to mechanisms on the bioanode[40]. *Azospira oryzae* was found to be a dominant exoelectrogenic microorganism containing a c-type cytochrome in a microbial fuel cell with acetate as the electron donor and Fe^{3+} as the electron acceptor.[36,41] *Stenotrophomonas* produced a maximum current density of 273 mA/m^2 through an extracellular electron transfer mechanism in a single-chamber microbial fuel cell.[42] It was also reported for its potential to degrade diesel derived hydrocarbons in a microbial fuel cell. *Desulfovibrio* directly transferred extracellular electrons to the anode through a multi-hemic cytochrome c protein in a mediator-free microbial fuel cell.[43–48] In another study, *Desulfovibrio* was reported to produce nanoscale, bacterial appendages for direct extracellular electron transfer.[49] *Desulfovibrio* was also

able to indirectly transfer electrons to the electrode using an inorganic electron mediator in a microbial fuel cell.[50,51]

Methanobacterium curvum, a chemolithotrophic methanogen, was enriched probably due to methanogenesis.[16,52,53] The cathodic potential at steady state was -56 mV,[16] which was below the redox potential needed for methanogenesis (*i.e.*, +50 mV).[54] The theoretical half-reaction potentials at the experimental conditions were 880 mV for selenate and 903 mV for selenite, respectively,[16] suggesting that selenate and selenite reductions were thermodynamically preferred compared to methanogenesis.

The microbial community in the cathodic effluent was similar to that of the biocathode, except for the increase of *Aminobacter sp.* and *Afipia sp.*. The similarity might be a result of the detachment of microbes from the biocathode to the surrounding liquid, while the difference could be explained by their specific ways to obtain electrons and energy: directly and indirectly from the cathode. Both *Aminobacter* and *Afipia* are in the order of *Rhizobiales*, a group of bacteria that are capable of accumulating poly-3-hydroxybutyric acid (PHB) as the extra energy source to survive in the cathodic liquid.[16,55,56]

The microbial community on the anode was dominated by *Geobacter soli* (30%) and *Pseudomonas sp. X-a5* (20%) (Figure 5). Both are well-known anode-respiring bacteria and can transfer electrons from bacteria to the anode either directly or indirectly by electron shuttles that they produce (*e.g.*, phenazine-based metabolites/redox mediators).[57–59] Those electron shuttles could also be used by other species on the electrode, such as *Clostridium sensu stricto 1* (6.5%) and

310 *Anaerolineaceae* (5.9%).[60,61] The microbial community on the anode and in the anodic effluent
311 were very different, which might be explained by whether they transfer electrons from acetate to
312 the electrode.
313
314 **3.4 Mechanisms of Extracellular SeNPs Production**
315 Although the entire biological pathway from selenate to SeNPs is unclear, the c-type cytochromes
316 (Cyt c) are agreed to be essential for electron transfer and redox reactions.[5,62] As shown in Figure
317 S5, Cyt c (1372 cm^{-1}) and elemental selenium (237 cm^{-1} and 255 cm^{-1}) were found on the surface
318 of the biocathode.[16,63] The Cyt c might transfer electrons from the biocathode to bacteria, and the
319 multi-heme in the c-type cytochromes might further shuttle electrons to selenate as an electron
320 acceptor.[64–66] The ability of Cyt c to reduce selenate to extracellular SeNPs (Equation 1) was
321 reported in the literature.[67–69]
322
$$SeO_4^{2-} + 1.5(Fe^{II}\text{-Cytochrome c}) + 8H^+ = 1.5(Fe^{III}\text{-Cytochrome c})^{4+} + Se^0 + 4H_2O \qquad \text{Equation 1}$$

323
324 Compared to the intracellular production of SeNPs, extracellular production eliminated the need
325 of transferring the electrons and selenate into the microbial cells (*i.e.*, cytoplasm), which saved
326 energy for the cell and was thereby preferred by the cells on the biocathode. As a result, bacteria
327 that were enriched on the biocathode preferred to produce extracellular SeNPs even if they have
328 the ability to produce both intracellular and extracellular SeNPs.
329
330 Producing extracellular Se^0 nanoparticles is more energy efficient than producing intracellular Se^0
331 nanoparticles for microorganisms on the biocathode. However, this is not necessarily true for

conventional reactors. Table 3 shows that the cellular energy cost for transporting e^- and selenate to the reductase for extracellular Se^0 nanoparticles production are less than the corresponding energy cost for intracellular Se^0 nanoparticles on biocathode.[70] Table S2 compares the transfer of e^- from the electron donor (*i.e.*, acetate) in the cytoplasm of bacteria to terminal reductases enabling intracellular and extracellular selenate reduction to Se^0 nanoparticles in the conventional reactor. While the selenate-transfer pathway is shorter for the extracellular than intracellular Se^0 nanoparticles production, the e^--transfer pathway is longer for extracellular than for intracellular Se^0 nanoparticles production.[69,71]

3.5 Environmental Implications

Similar to Se reduction in conventional bioreactors, particulate metals and metalloids such as Cu, Pd, Au, Cr and Te were reported to form both intracellularly and extracellularly during conventional biological reduction. For example, Kimber et al. found Cu(II) could be reduced to Cu nanoparticles by *Shewanella oneidensis*, but the produced Cu nanoparticles were predominantly located inside the bacterial cells.[72] Deplanche et al. reported the reduction of Pd(II) to Pd nanoparticles by *Escherichia coli*, but the produced Pd nanoparticles were located both intracellularly and extracellularly.[73] Konishi et al. found the intracellular production of Au nanoparticles by *Shewanella algae* from $AuCl_4^-$.[74] Gong et al. found more intracellular than extracellular particulate Cr(III) were produced through the reduction of dissolved Cr(VI) by *Geobacter sulfurreducens* PCA.[75] Ramos-Ruiz et al. report both intracellular and extracellular Te nanoparticles using a methanogenic microbial consortium.[76] The extracellular redox reaction could be potentially applied to recover these metals and metalloids by minimizing the production

of intracellular particulates. Future studies at the enzyme (e.g., cytochrome c) level and cellular (pure species) level are needed to fully support the conclusion on the mechanisms.

This study reports the potential application of biocathode based synthesis of extracellular elemental selenium and removal and recovery of selenium from contaminated wastewater. The major five new aspects of this study's contribution are as follows. First, we demonstrated that the percentage of cells producing intracellular selenium nanoparticles was only 1-3% on the biocathode, but 10-99% in the conventional reactors. This includes direct comparison through our experiments and indirect comparison through literature review. The STEM-EDX results were used to provide a direct evidence of more extracellular selenium nanoparticles production on the biocathode than in the conventional reactor. Second, we demonstrated that different biomass seeds used on biocathode led to similar results: producing much more extracellular selenium nanoparticles than intracellular selenium nanoparticles. Third, the microbial community analysis results show that the dominant microbial species on the biocathode were also present in conventional bioreactors, but they changed their behavior on the biocathode by preferentially producing more extracellular selenium nanoparticles. Finally, we further explained the mechanisms: Bacteria prefer to produce extracellular selenium nanoparticles on the biocathode, but intracellular selenium nanoparticles in conventional reactors because doing so saves their cellular energy.

Supporting Information

Detailed description of sample preparation for SEM and TEM, extraction of DNA, and 16S rRNA gene sequencing analysis with supporting tables and figures.

Notes

The authors declare no competing financial interest.

Acknowledgements

This work was supported by National Science Foundation through award #2029682 to Florida State University. The authors greatly thank Dr. Eric Lochner, Dr. Duncan Sousa, Dr. Yan Xin, Mr. Grayson Platt, and Mr. Darryl Trickey at Florida State University for providing technical support in the SEM, TEM, and STEM imaging, Dr. Jin Gyu Park at the High-Performance Materials Institute, Florida State University for providing help in Raman Spectroscopy analysis, and Dr. Stefan J. Green at the University of Illinois at Chicago for 16S rRNA sequencing. The SEM work was performed at the Condensed Matter and Material Physics facilities, Florida State University. The TEM work was performed at the Biological Science Imaging Resource, Florida State University using the instrument, Hitachi HT7800, which was funded from NSF through grant #2017869. The STEM work was performed at the National High Magnetic Field Laboratory, using the STEM supported by National Science Foundation Cooperative Agreement No. DMR-1644779 and the State of Florida.

References

(1) USEPA. Drinking Water Contaminants: National Primary Drinking Water Regulations. *US EPA website http//water.epa.gov/drink/contaminants/index.cfm* **2015**, No. 18540.

(2) Kharaka, Y. K.; Ambats, G.; Presser, T. S.; Davis, R. A. Removal of Selenium from Contaminated Agricultural Drainage Water by Nanofiltration Membranes. *Appl. Geochemistry* **1996**, *11* (6). https://doi.org/10.1016/S0883-2927(96)00044-3.

(3) Lenz, M.; Lens, P. N. L. The Essential Toxin: The Changing Perception of Selenium in Environmental Sciences. *Sci. Total Environ.* **2009**, *407* (12). https://doi.org/10.1016/j.scitotenv.2008.07.056.

(4) Oremland, R. S.; Hollibaugh, J. T.; Maest, A. S.; Presser, T. S.; Miller, L. G.; Culbertson, C. W. Selenate Reduction to Elemental Selenium by Anaerobic Bacteria in Sediments and Culture: Biogeochemical Significance of a Novel, Sulfate-Independent Respiration. *Appl. Environ. Microbiol.* **1989**, *55* (9). https://doi.org/10.1128/aem.55.9.2333-2343.1989.

(5) Nancharaiah, Y. V.; Lens, P. N. L. Selenium Biomineralization for Biotechnological Applications. *Trends in Biotechnology*. 2015. https://doi.org/10.1016/j.tibtech.2015.03.004.

(6) Zhang, Z.; Adedeji, I.; Chen, G.; Tang, Y. Chemical-Free Recovery of Elemental Selenium from Selenate-Contaminated Water by a System Combining a Biological Reactor, a Bacterium-Nanoparticle Separator, and a Tangential Flow Filter. *Environ. Sci. Technol.* **2018**, *52* (22). https://doi.org/10.1021/acs.est.8b04544.

(7) Lai, C. Y.; Song, Y.; Wu, M.; Lu, X.; Wang, Y.; Yuan, Z.; Guo, J. Microbial Selenate Reduction in Membrane Biofilm Reactors Using Ethane and Propane as Electron Donors.

Water Res. **2020**, *183*. https://doi.org/10.1016/j.watres.2020.116008.

(8) Sinharoy, A.; Lens, P. N. L. Biological Removal of Selenate and Selenite from Wastewater: Options for Selenium Recovery as Nanoparticles. *Current Pollution Reports*. 2020. https://doi.org/10.1007/s40726-020-00146-4.

(9) Macy, J. M.; Lawson, S.; DeMoll-Decker, H. Bioremediation of Selenium Oxyanions in San Joaquin Drainage Water Using Thauera Selenatis in a Biological Reactor System. *Appl. Microbiol. Biotechnol.* **1993**, *40* (4). https://doi.org/10.1007/BF00175752.

(10) Soda, S.; Kashiwa, M.; Kagami, T.; Kuroda, M.; Yamashita, M.; Ike, M. Laboratory-Scale Bioreactors for Soluble Selenium Removal from Selenium Refinery Wastewater Using Anaerobic Sludge. *Desalination* **2011**, *279* (1–3). https://doi.org/10.1016/j.desal.2011.06.031.

(11) Staicu, L. C.; van Hullebusch, E. D.; Lens, P. N. L. Production, Recovery and Reuse of Biogenic Elemental Selenium. *Environmental Chemistry Letters*. 2015. https://doi.org/10.1007/s10311-015-0492-8.

(12) Stillings, L.L., Selenium, chap. Q of Schulz, K.J., DeYoung, J.H., Jr., Seal, R.R., II, and Bradley, D.C., E. *Critical Mineral Resources of the United States—Economic and Environmental Geology and Prospects for Future Supply*; 2017.

(13) Moss, R.L., Tzimas, E., Kara, H., Willis, P., & Kooroshy, J. *Critical Metals in Strategic Energy Technologies Assessing Rare Metals as Supply-Chain Bottlenecks in Low-Carbon Energy Technologies (EUR--24884-EN-2011)*; Netherlands, 2011.

(14) Liang, X.; Gadd, G. M. Metal and Metalloid Biorecovery Using Fungi. *Microb.*

Biotechnol. **2017**, *10* (5). https://doi.org/10.1111/1751-7915.12767.

(15) Graedel, T. E.; Harper, E. M.; Nassar, N. T.; Nuss, P.; Reck, B. K.; Turner, B. L. Criticality of Metals and Metalloids. *Proc. Natl. Acad. Sci. U. S. A.* **2015**, *112* (14). https://doi.org/10.1073/pnas.1500415112.

(16) Zhang, Z.; Chen, G.; Tang, Y. Towards Selenium Recovery: Biocathode Induced Selenate Reduction to Extracellular Elemental Selenium Nanoparticles. *Chem. Eng. J.* **2018**, *351*. https://doi.org/10.1016/j.cej.2018.06.172.

(17) Avendaño, R.; Chaves, N.; Fuentes, P.; Sánchez, E.; Jiménez, J. I.; Chavarría, M. Production of Selenium Nanoparticles in Pseudomonas Putida KT2440. *Sci. Rep.* **2016**, *6*. https://doi.org/10.1038/srep37155.

(18) Shakibaie, M.; Khorramizadeh, M. R.; Faramarzi, M. A.; Sabzevari, O.; Shahverdi, A. R. Biosynthesis and Recovery of Selenium Nanoparticles and the Effects on Matrix Metalloproteinase-2 Expression. *Biotechnol. Appl. Biochem.* **2010**, *56* (1). https://doi.org/10.1042/ba20100042.

(19) Sonkusre, P.; Nanduri, R.; Gupta, P.; Cameotra, S. S. Improved Extraction of Intracellular Biogenic Selenium Nanoparticles and Their Specificity for Cancer Chemoprevention. *J. Nanomedicine Nanotechnol.* **2014**, *5* (2). https://doi.org/10.4172/2157-7439.1000194.

(20) Altringer, P. B.; Lien, R. H.; Gardner, K. R. Biological and Chemical Selenium Removal from Precious Metals Solutions; 1991.

(21) Lawson, S.; Macy, J. M. Bioremediation of Selenite in Oil Refinery Wastewater. *Appl. Microbiol. Biotechnol.* **1995**, *43* (4). https://doi.org/10.1007/BF00164785.

(22) Lai, C. Y.; Yang, X.; Tang, Y.; Rittmann, B. E.; Zhao, H. P. Nitrate Shaped the Selenate-Reducing Microbial Community in a Hydrogen-Based Biofilm Reactor. *Environ. Sci. Technol.* **2014**, *48* (6). https://doi.org/10.1021/es4053939.

(23) Hunter, W. J. Removing Selenate from Groundwater with a Vegetable Oil-Based Biobarrier. *Curr. Microbiol.* **2006**, *53* (3). https://doi.org/10.1007/s00284-006-0119-1.

(24) Van Ginkel SW, Yang Z, Kim BO, Sholin M, R. B. Effect of PH on Nitrate and Selenate Reduction in Flue Gas Desulfurization Brine Using the H2-Based Membrane Biofilm Reactor (MBfR). *Water Sci Technol* **2011**, *63(12)*, 2923–2928.

(25) Zhang, Z.; Tang, Y. Comparing Methods for Measuring Dissolved and Particulate Selenium in Water. *J. Water Environ. Technol.* **2020**, *18* (4). https://doi.org/10.2965/jwet.20-003.

(26) Lefebvre, O.; Al-Mamun, A.; Ng, H. Y. A Microbial Fuel Cell Equipped with a Biocathode for Organic Removal and Denitrification. *Water Sci. Technol.* **2008**, *58* (4). https://doi.org/10.2166/wst.2008.343.

(27) Tandukar, M.; Huber, S. J.; Onodera, T.; Pavlostathis, S. G. Biological Chromium(VI) Reduction in the Cathode of a Microbial Fuel Cell. *Environ. Sci. Technol.* **2009**, *43* (21). https://doi.org/10.1021/es9014184.

(28) Negi, B. B.; Sinharoy, A.; Pakshirajan, K. Selenite Removal from Wastewater Using Fungal Pelleted Airlift Bioreactor. *Environ. Sci. Pollut. Res.* **2020**, *27* (1). https://doi.org/10.1007/s11356-019-06946-6.

(29) Wadgaonkar, S. L.; Mal, J.; Nancharaiah, Y. V.; Maheshwari, N. O.; Esposito, G.; Lens,

P. N. L. Formation of Se(0), Te(0), and Se(0)–Te(0) Nanostructures during Simultaneous Bioreduction of Selenite and Tellurite in a UASB Reactor. *Appl. Microbiol. Biotechnol.* **2018**, *102* (6). https://doi.org/10.1007/s00253-018-8781-3.

(30) Viamajala, S.; Bereded-Samuel, Y.; Apel, W. A.; Petersen, J. N. Selenite Reduction by a Denitrifying Culture: Batch- and Packed-Bed Reactor Studies. *Appl. Microbiol. Biotechnol.* **2006**, *71* (6). https://doi.org/10.1007/s00253-005-0276-3.

(31) Sinharoy, A.; Saikia, S.; Pakshirajan, K. Biological Removal of Selenite from Wastewater and Recovery as Selenium Nanoparticles Using Inverse Fluidized Bed Bioreactor. *J. Water Process Eng.* **2019**, *32*. https://doi.org/10.1016/j.jwpe.2019.100988.

(32) Ontiveros-Valencia, A.; Penton, C. R.; Krajmalnik-Brown, R.; Rittmann, B. E. Hydrogen-Fed Biofilm Reactors Reducing Selenate and Sulfate: Community Structure and Capture of Elemental Selenium within the Biofilm. *Biotechnol. Bioeng.* **2016**, *113* (8). https://doi.org/10.1002/bit.25945.

(33) Jain, R.; Matassa, S.; Singh, S.; van Hullebusch, E. D.; Esposito, G.; Lens, P. N. L. Reduction of Selenite to Elemental Selenium Nanoparticles by Activated Sludge. *Environ. Sci. Pollut. Res.* **2016**, *23* (2). https://doi.org/10.1007/s11356-015-5138-7.

(34) Piacenza, E.; Presentato, A.; Ferrante, F.; Cavallaro, G.; Alduina, R.; Martino, D. F. C. Biogenic Selenium Nanoparticles: A Fine Characterization to Unveil Their Thermodynamic Stability. *Nanomaterials* **2021**, *11* (5). https://doi.org/10.3390/nano11051195.

(35) Xin, X. F.; Kvitko, B.; He, S. Y. Pseudomonas Syringae: What It Takes to Be a Pathogen. *Nature Reviews Microbiology*. 2018. https://doi.org/10.1038/nrmicro.2018.17.

(36) Hunter, W. J. An Azospira Oryzae (Syn Dechlorosoma Suillum) Strain That Reduces Selenate and Selenite to Elemental Red Selenium. *Curr. Microbiol.* **2007**, *54* (5). https://doi.org/10.1007/s00284-006-0474-y.

(37) Brooke, J. S. Stenotrophomonas Maltophilia: An Emerging Global Opportunistic Pathogen. *Clinical Microbiology Reviews*. 2012. https://doi.org/10.1128/CMR.00019-11.

(38) Compeau, G. C.; Bartha, R. Sulfate-Reducing Bacteria: Principal Methylators of Mercury in Anoxic Estuarine Sediment. *Appl. Environ. Microbiol.* **1985**, *50* (2). https://doi.org/10.1128/aem.50.2.498-502.1985.

(39) Wenzel, M.; Dekker, M. P.; Wang, B.; Burggraaf, M. J.; Bitter, W.; van Weering, J. R. T.; Hamoen, L. W. A Flat Embedding Method for Transmission Electron Microscopy Reveals an Unknown Mechanism of Tetracycline. *Commun. Biol.* **2021**, *4* (1). https://doi.org/10.1038/s42003-021-01809-8.

(40) Kumar, R.; Singh, L.; Zularisam, A. W. Exoelectrogens: Recent Advances in Molecular Drivers Involved in Extracellular Electron Transfer and Strategies Used to Improve It for Microbial Fuel Cell Applications. *Renewable and Sustainable Energy Reviews*. 2016. https://doi.org/10.1016/j.rser.2015.12.029.

(41) Becerril-Varela, K.; Serment-Guerrero, J. H.; Manzanares-Leal, G. L.; Ramírez-Durán, N.; Guerrero-Barajas, C. Generation of Electrical Energy in a Microbial Fuel Cell Coupling Acetate Oxidation to Fe3+ Reduction and Isolation of the Involved Bacteria. *World J. Microbiol. Biotechnol.* **2021**, *37* (6). https://doi.org/10.1007/s11274-021-03077-4.

(42) Venkidusamy, K.; Megharaj, M. Identification of Electrode Respiring,

Hydrocarbonoclastic Bacterial Strain Stenotrophomonas Maltophilia MK2 Highlights the Untapped Potential for Environmental Bioremediation. *Front. Microbiol.* **2016**, *7* (DEC). https://doi.org/10.3389/fmicb.2016.01965.

(43) Kang, C. S.; Eaktasang, N.; Kwon, D. Y.; Kim, H. S. Enhanced Current Production by Desulfovibrio Desulfuricans Biofilm in a Mediator-Less Microbial Fuel Cell. *Bioresour. Technol.* **2014**, *165* (C). https://doi.org/10.1016/j.biortech.2014.03.148.

(44) Arbour, T. J. Cultivating and Characterizing Electroactive Microbial Communities Using Bioelectrochemical Systems and Metagenomics, University of California, Berkeley, 2017.

(45) Barton, L. L.; Tomei-Torres, F. A.; Xu, H.; Zocco, T. Nanoparticles Formed by Microbial Metabolism of Metals and Minerals. In *Nanomicrobiology: Physiological and Environmental Characteristics*; 2014; Vol. 9781493916672. https://doi.org/10.1007/978-1-4939-1667-2_7.

(46) Chow, V. Te; Maidment, D. R.; Mays, L. W. *Applied Hydrology (Letters)*; 1988.

(47) Lu, L.; Lobo, F. L.; Xing, D.; Ren, Z. J. Active Harvesting Enhances Energy Recovery and Function of Electroactive Microbiomes in Microbial Fuel Cells. *Appl. Energy* **2019**, *247*. https://doi.org/10.1016/j.apenergy.2019.04.074.

(48) Zhang, L.; Fu, G.; Zhang, Z. Electricity Generation and Microbial Community in Long-Running Microbial Fuel Cell for High-Salinity Mustard Tuber Wastewater Treatment. *Bioelectrochemistry* **2019**, *126*. https://doi.org/10.1016/j.bioelechem.2018.11.002.

(49) Eaktasang, N.; Kang, C. S.; Lim, H.; Kwean, O. S.; Cho, S.; Kim, Y.; Kim, H. S. Production of Electrically-Conductive Nanoscale Filaments by Sulfate-Reducing Bacteria

in the Microbial Fuel Cell. *Bioresour. Technol.* **2016**, *210*. https://doi.org/10.1016/j.biortech.2015.12.090.

(50) Zhao, F.; Rahunen, N.; Varcoe, J. R.; Chandra, A.; Avignone-Rossa, C.; Thumser, A. E.; Slade, R. C. T. Activated Carbon Cloth as Anode for Sulfate Removal in a Microbial Fuel Cell. *Environ. Sci. Technol.* **2008**, *42* (13). https://doi.org/10.1021/es8003766.

(51) Miran, W.; Jang, J.; Nawaz, M.; Shahzad, A.; Jeong, S. E.; Jeon, C. O.; Lee, D. S. Mixed Sulfate-Reducing Bacteria-Enriched Microbial Fuel Cells for the Treatment of Wastewater Containing Copper. *Chemosphere* **2017**, *189*. https://doi.org/10.1016/j.chemosphere.2017.09.048.

(52) Wagner, R. C. Methane Production and Methanogenic Communities in Microbial Electrolysis Cells, Anodic Potential Influence on Microbial Fuel Cells, and a Method to Entrap Microbes on an Electrode, The Pennsylvania State University, 2012.

(53) Na, B. K.; Tae, S. H.; Sung, H. L.; Dong, H. J.; Byung, I. S.; Doo, H. P. Development of Bioreactors for Enrichment of Chemolithotrophic Methanogen and Methane Production. *Korean J. Microbiol. Biotechnol.* **2007**, *35* (1).

(54) Fetzer, S.; Conrad, R. Effect of Redox Potential on Methanogenesis by Methanosarcina Barkeri. *Arch. Microbiol.* **1993**, *160* (2). https://doi.org/10.1007/BF00288711.

(55) KONDO, T.; TSUNEDA, S.; EBIE, Y.; INAMORI, Y.; XU, K. Characterization of the Microbial Community in the Anaerobic/Oxic/Anoxic Process Combined with Sludge Ozonation and Phosphorus Adsorption. *J. Water Environ. Technol.* **2009**, *7* (3). https://doi.org/10.2965/jwet.2009.155.

(56) Wang, J.; Chu, L. Biological Nitrate Removal from Water and Wastewater by Solid-Phase Denitrification Process. *Biotechnology Advances*. 2016. https://doi.org/10.1016/j.biotechadv.2016.07.001.

(57) Rabaey, K.; Boon, N.; Höfte, M.; Verstraete, W. Microbial Phenazine Production Enhances Electron Transfer in Biofuel Cells. *Environ. Sci. Technol.* **2005**, *39* (9). https://doi.org/10.1021/es048563o.

(58) Pham, T. H.; Boon, N.; De Maeyer, K.; Höfte, M.; Rabaey, K.; Verstraete, W. Use of Pseudomonas Species Producing Phenazine-Based Metabolites in the Anodes of Microbial Fuel Cells to Improve Electricity Generation. *Appl. Microbiol. Biotechnol.* **2008**, *80* (6). https://doi.org/10.1007/s00253-008-1619-7.

(59) Yun, H.; Liang, B.; Kong, D.; Wang, A. Improving Biocathode Community Multifunctionality by Polarity Inversion for Simultaneous Bioelectroreduction Processes in Domestic Wastewater. *Chemosphere* **2018**, *194*. https://doi.org/10.1016/j.chemosphere.2017.12.030.

(60) Hao, L.; Zhang, B.; Cheng, M.; Feng, C. Effects of Various Organic Carbon Sources on Simultaneous V(V) Reduction and Bioelectricity Generation in Single Chamber Microbial Fuel Cells. *Bioresour. Technol.* **2016**, *201*. https://doi.org/10.1016/j.biortech.2015.11.060.

(61) Dessì, P.; Porca, E.; Haavisto, J.; Lakaniemi, A. M.; Collins, G.; Lens, P. N. L. Composition and Role of the Attached and Planktonic Microbial Communities in Mesophilic and Thermophilic Xylose-Fed Microbial Fuel Cells. *RSC Adv.* **2018**, *8* (6). https://doi.org/10.1039/c7ra12316g.

(62) Bond, D. R.; Strycharz-Glaven, S. M.; Tender, L. M.; Torres, C. I. On Electron Transport

through Geobacter Biofilms. *ChemSusChem* **2012**, *5* (6). https://doi.org/10.1002/cssc.201100748.

(63) Virdis, B.; Millo, D.; Donose, B. C.; Batstone, D. J. Real-Time Measurements of the Redox States of c-Type Cytochromes in Electroactive Biofilms: A Confocal Resonance Raman Microscopy Study. *PLoS One* **2014**, *9* (2). https://doi.org/10.1371/journal.pone.0089918.

(64) Busalmen, J. P.; Esteve-Núñez, A.; Berná, A.; Feliu, J. M. C-Type Cytochromes Wire Electricity-Producing Bacteria to Electrodes. *Angew. Chemie - Int. Ed.* **2008**, *47* (26). https://doi.org/10.1002/anie.200801310.

(65) Wu, J. F.; Xu, M. Q.; Zhao, G. C. Graphene-Based Modified Electrode for the Direct Electron Transfer of Cytochrome c and Biosensing. *Electrochem. commun.* **2010**, *12* (1). https://doi.org/10.1016/j.elecom.2009.11.020.

(66) Esteve-Núñez, A.; Sosnik, J.; Visconti, P.; Lovley, D. R. Fluorescent Properties of C-Type Cytochromes Reveal Their Potential Role as an Extracytoplasmic Electron Sink in Geobacter Sulfurreducens. *Environ. Microbiol.* **2008**, *10* (2). https://doi.org/10.1111/j.1462-2920.2007.01470.x.

(67) Myers, C. R.; Myers, J. M. Localization of Cytochromes to the Outer Membrane of Anaerobically Grown Shewanella Putrefaciens MR-1. *J. Bacteriol.* **1992**, *174* (11). https://doi.org/10.1128/jb.174.11.3429-3438.1992.

(68) A. Abdelouas, W. L. Gong, W. Lutze, J. A.; Shelnu, R, F. and I. M. Using Cytochrome c 3 to Make Selenium Nanowires. *Chem. Mater. 1* **2000**, *12(6)*, 1510–1512.

(69) Li, D. B.; Cheng, Y. Y.; Wu, C.; Li, W. W.; Li, N.; Yang, Z. C.; Tong, Z. H.; Yu, H. Q. Selenite Reduction by Shewanella Oneidensis MR-1 Is Mediated by Fumarate Reductase in Periplasm. *Sci. Rep.* **2014**, *4*. https://doi.org/10.1038/srep03735.

(70) Zou, L.; Zhu, F.; Long, Z. er; Huang, Y. Bacterial Extracellular Electron Transfer: A Powerful Route to the Green Biosynthesis of Inorganic Nanomaterials for Multifunctional Applications. *Journal of Nanobiotechnology*. 2021. https://doi.org/10.1186/s12951-021-00868-7.

(71) Von Canstein, H.; Ogawa, J.; Shimizu, S.; Lloyd, J. R. Secretion of Flavins by Shewanella Species and Their Role in Extracellular Electron Transfer. *Appl. Environ. Microbiol.* **2008**, *74* (3). https://doi.org/10.1128/AEM.01387-07.

(72) Kimber, R. L.; Lewis, E. A.; Parmeggiani, F.; Smith, K.; Bagshaw, H.; Starborg, T.; Joshi, N.; Figueroa, A. I.; van der Laan, G.; Cibin, G.; Gianolio, D.; Haigh, S. J.; Pattrick, R. A. D.; Turner, N. J.; Lloyd, J. R. Biosynthesis and Characterization of Copper Nanoparticles Using Shewanella Oneidensis: Application for Click Chemistry. *Small* **2018**, *14* (10). https://doi.org/10.1002/smll.201703145.

(73) Deplanche, K.; Caldelari, I.; Mikheenko, I. P.; Sargent, F.; Macaskie, L. E. Involvement of Hydrogenases in the Formation of Highly Catalytic Pd(0) Nanoparticles by Bioreduction of Pd(II) Using Escherichia Coli Mutant Strains. *Microbiology* **2010**, *156* (9). https://doi.org/10.1099/mic.0.036681-0.

(74) Konishi, Y.; Tsukiyama, T.; Ohno, K.; Saitoh, N.; Nomura, T.; Nagamine, S. Intracellular Recovery of Gold by Microbial Reduction of AuCl 4- Ions Using the Anaerobic Bacterium Shewanella Algae. *Hydrometallurgy* **2006**, *81* (1).

https://doi.org/10.1016/j.hydromet.2005.09.006.

(75) Gong, Y.; Werth, C. J.; He, Y.; Su, Y.; Zhang, Y.; Zhou, X. Intracellular versus Extracellular Accumulation of Hexavalent Chromium Reduction Products by Geobacter Sulfurreducens PCA. *Environ. Pollut.* **2018**, *240*. https://doi.org/10.1016/j.envpol.2018.04.046.

(76) Ramos-Ruiz, A.; Field, J. A.; Wilkening, J. V.; Sierra-Alvarez, R. Recovery of Elemental Tellurium Nanoparticles by the Reduction of Tellurium Oxyanions in a Methanogenic Microbial Consortium. *Environ. Sci. Technol.* **2016**, *50* (3). https://doi.org/10.1021/acs.est.5b04074.

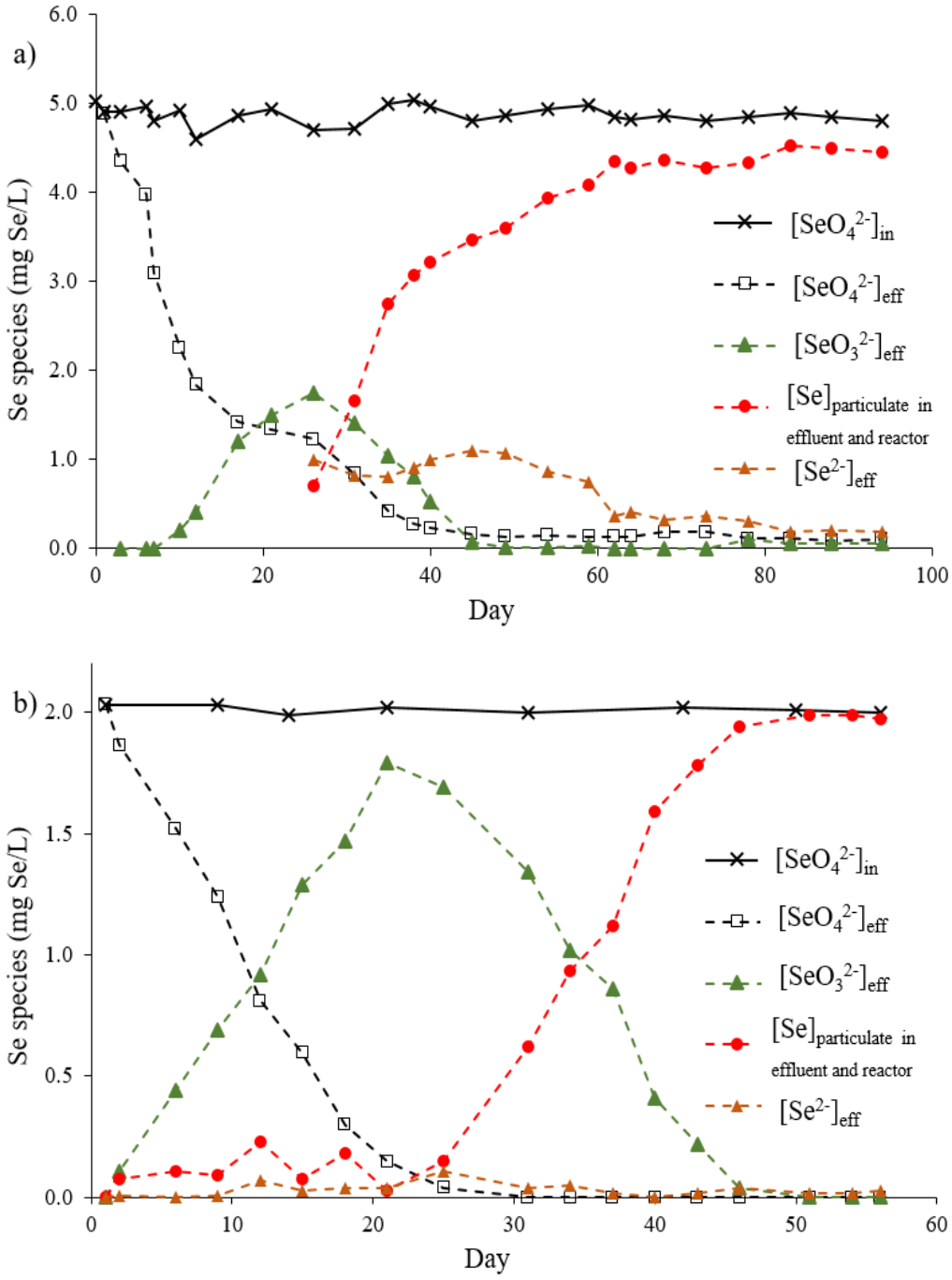

640

641
642 **Figure 1.** Selenate reduction in the cathodic chamber of BEC_2 (a) and BEC_3 (b).
643

Inoculum

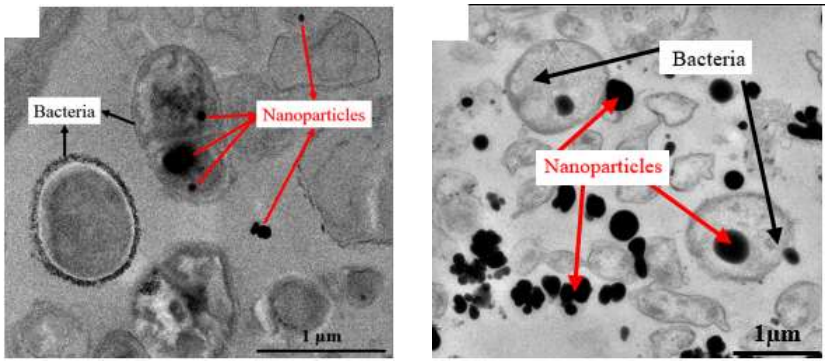

BEC_2

(Left: cathodic effluent,

Right: biocathode)

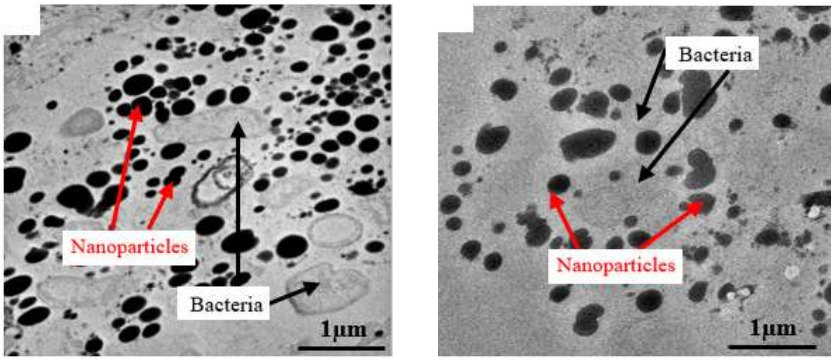

BEC_3

(Left: cathodic effluent,

Right: biocathode)

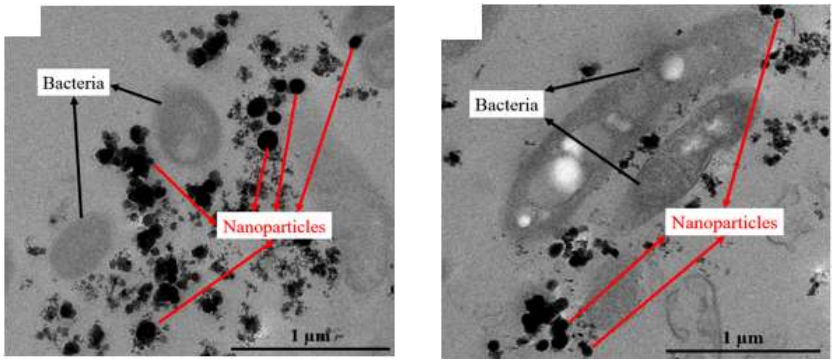

Conventional reactor control

Left: reactor effluent,

Right: in the reactor)

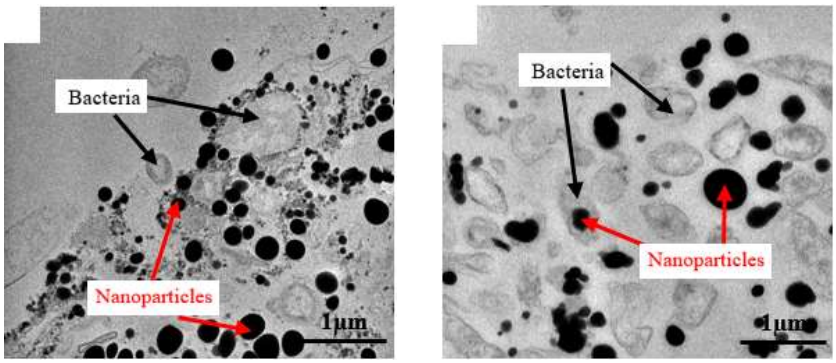

644 **Figure 2.** Representative thin-section TEM images of the particle mixtures in the inoculum,
645 BEC_2, BEC_3, and the conventional reactor control.

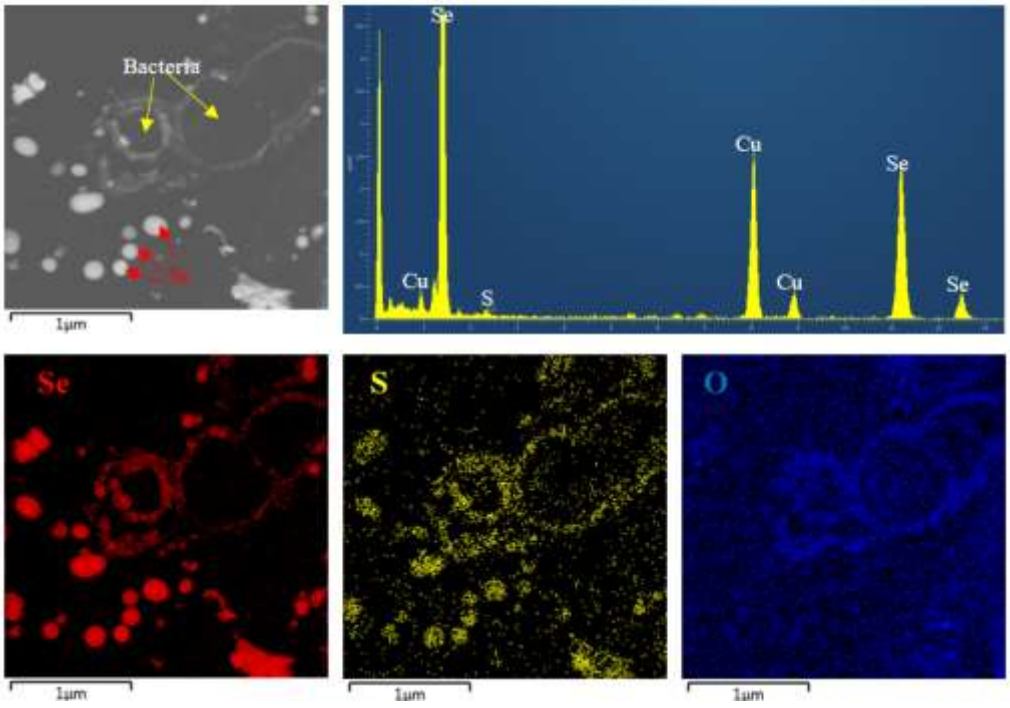

a) Biocathode from BEC_2

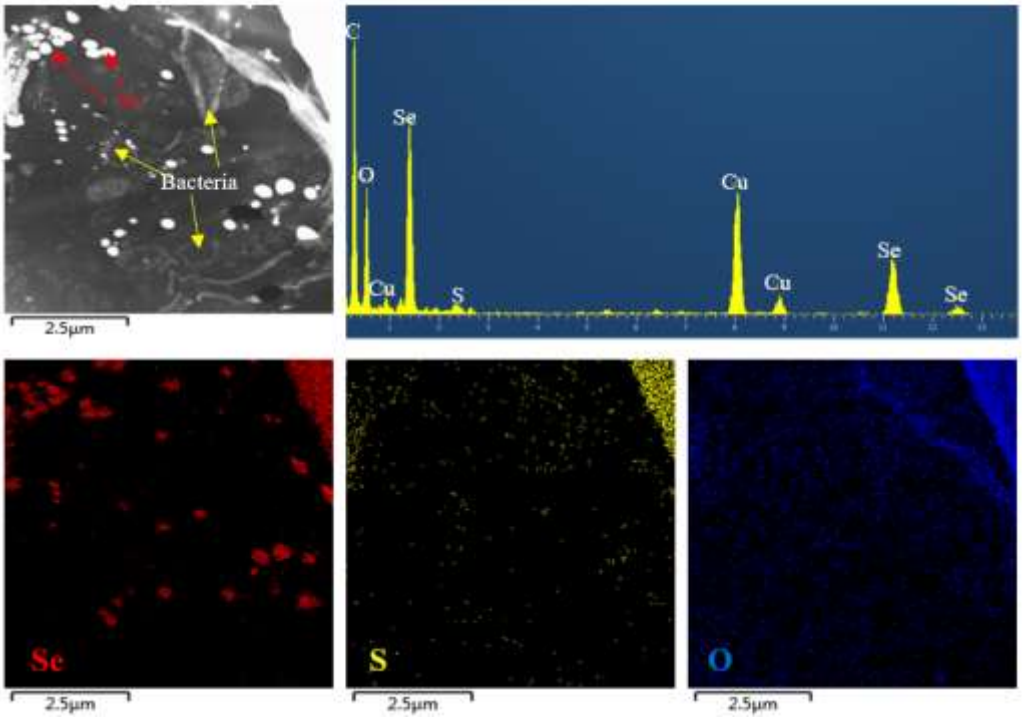

b) The conventional reactor control

646 **Figure 3.** Representative STEM image with EDX spectra (first row, left) and EDX mapping
647 spectra (second row) for particulates on the biocathode of BEC_2 reactor (a) and the conventional
648 reactor control (b) at steady state. Notes: Se was the absolutely predominant element of the
649 nanoparticles; Cu represented the copper grid used for holding the samples.

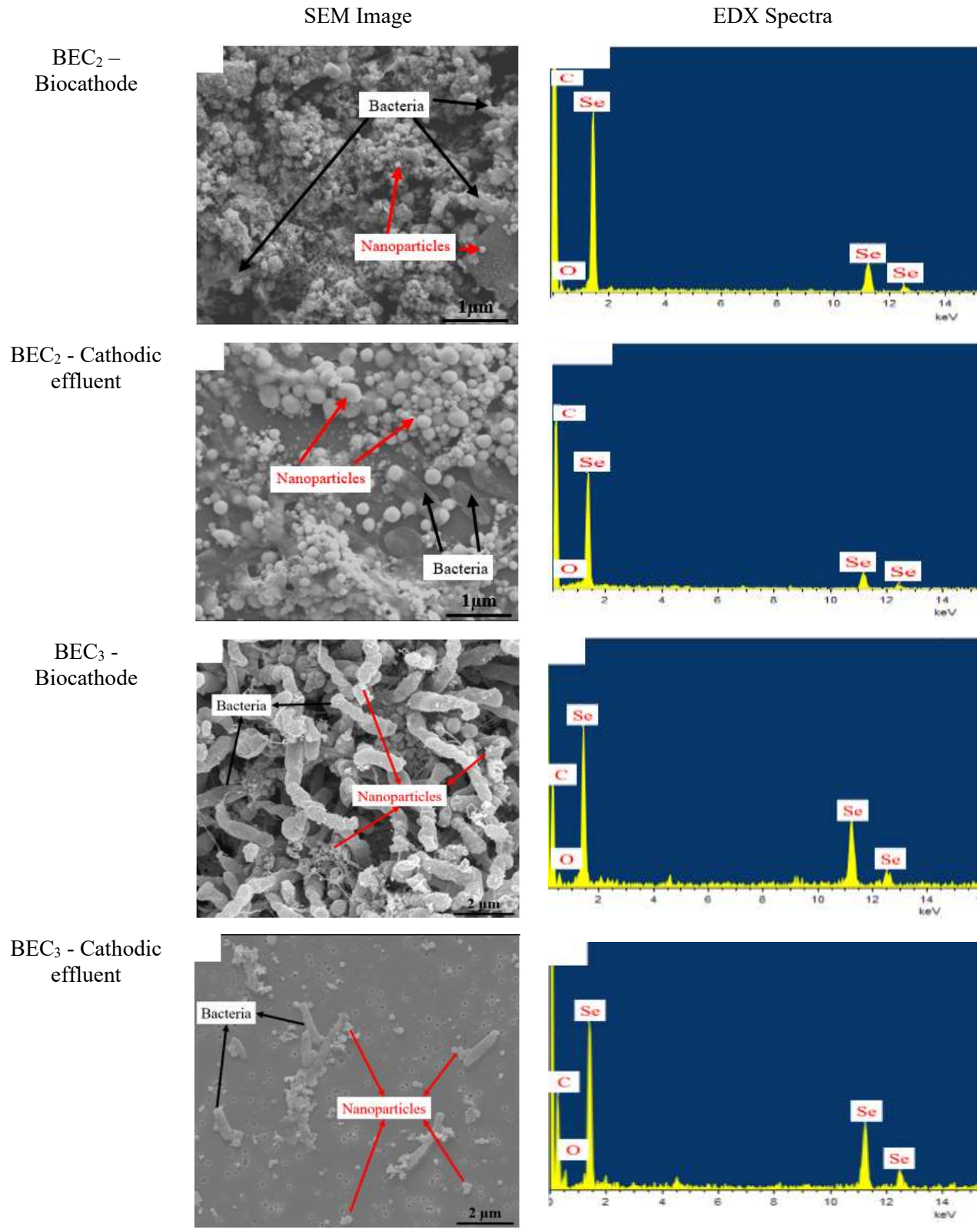

650 **Figure 4.** Representative SEM images and EDX spectra for the elemental selenium nanoparticles (SeNPs)
651 produced on the biocathode (30 images) and cathode effluent (30 images) of BEC_2 and BEC_3 reactors.

652

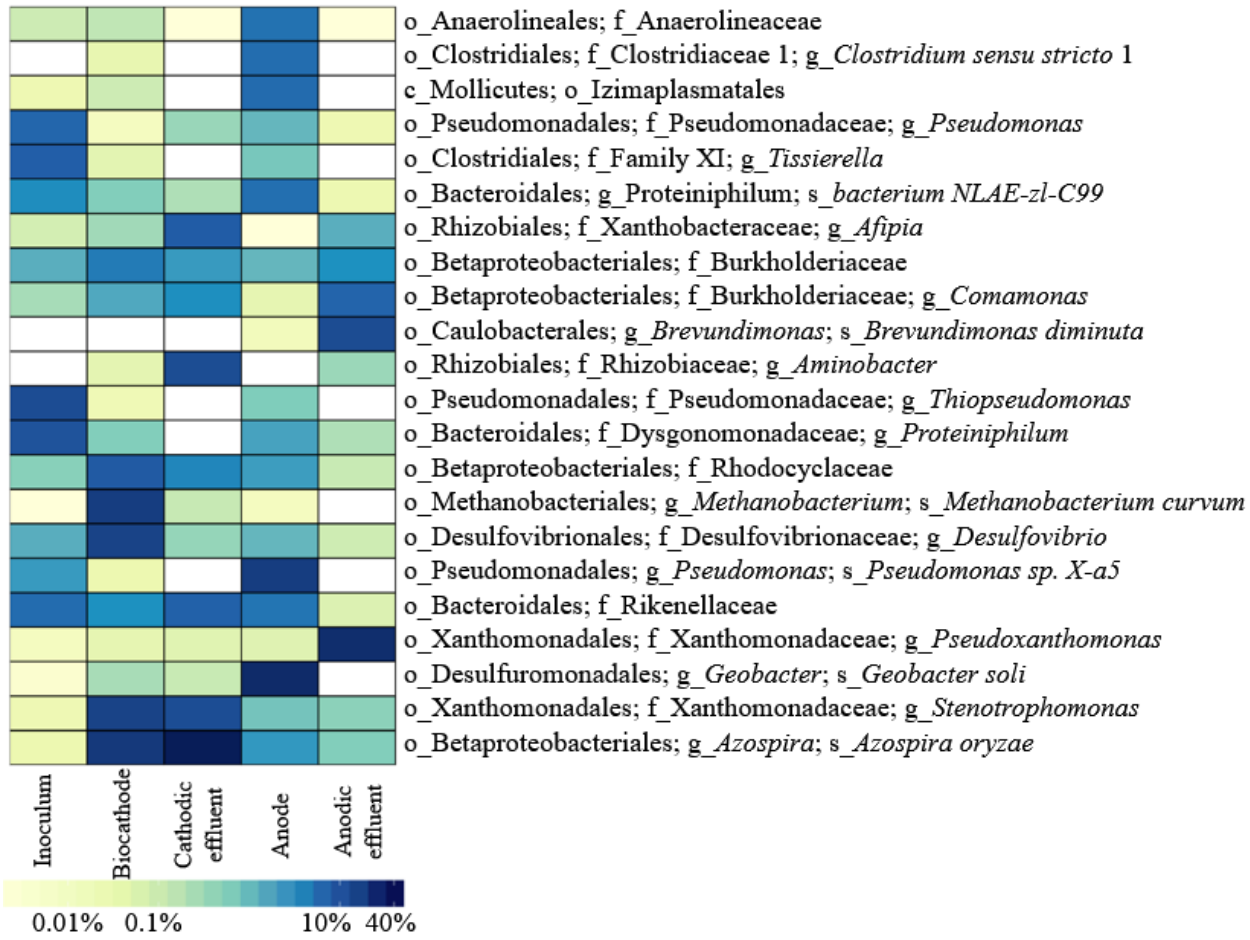

Figure 5. Heatmap showing relative abundance of dominating OTUs in the microbial community from BEC_1. Only the OTUs with a relative abundance of >5% in at least one of the five samples are shown. Notes: c=class, o=order, f=family, g=genus, and s=species.

658 **Table 1.** Comparison of BEC_1, BEC_2, BEC_3, and three controls during steady state

	Parameters	BEC_1 (Zhang et al., 2018)[16]	BEC_2 (this study)	BEC_3 (this study)	Sterile cathode control (Zhang et al., 2018)[16]	Open circuit control (Zhang et al., 2018)[16]	Conventional reactor control (this study)
Operating conditions	Inoculum	activated sludge + landfill leachate	activated sludge	activated sludge	activated sludge + landfill leachate	activated sludge + landfill leachate	activated sludge
	Flow rate (mL/day)	200	200	75	200	200	430
	SeO_4^{2-} surface loading rate (mg Se/m^2-day)	330	330	50	330	330	330
	Acetate surface loading rate (mg C/m^2-day)	660	660	250	660	660	660
Reactor performance	SeO_4^{2-} in influent (mg Se/L)	~5.0	~5.0	~2.0	~5.0	~5.0	~5.0
	SeO_4^{2-} in effluent (mg Se/L)	BQL[1]	BQL	BQL	~5.0	~5.0	BQL
	SeO_3^{2-} in effluent (mg Se/L)	~0.05	BQL	BQL	BQL	BQL	BQL
	Se^{2-} in effluent (mg Se/L)	~0.05	~0.08	~0.05	BQL	BQL	~0.04
	Particulate Se (mg Se/L)	~5.0	~4.5	~2.0	BQL	BQL	~4.8
	Acetate in influent (mg C/L)	~10	~10	~10	~10	~10	~10
	Acetate in effluent (mg C/L)	~4.0	~0.9	~4.0	~10	~10	~3.0
	SO_4^{2-} in influent (mg S/L)	~5.0	~5.0	~5.0	~5.0	~5.0	~5.0
	SO_4^{2-} in anodic effluent (mg S/L)	~4.7	~4.0	~4.6	~5.0	~5.0	~4.7
	SO_4^{2-} in cathodic effluent (mg S/L)	~4.9	~4.8	~4.9	~5.0	~5.0	-
	Voltage (mV)	~26	~12	~6.6	~0.1	0.00	-
	Current (mA)	~0.26	~0.12	~0.07	~0.001	0.00	-
	Power density (mW/m^2)	~2.2	~0.48	~0.15	0.00	0.00	-
	Current density (mA/m^2)	~86	~40	~22	0.30	0.00	-

Notes: [1]BQL = below quantification limit (< 0.02 mg/L); See Table 2 for the production percentage of intracellular versus extracellular selenium.

659

660 **Table 2.** Percentages of microbial cells having intracellular dense and spherical nanoparticles
661 per TEM images in various reactors

	Percentages of cells having intracellular nanoparticles	References
BEC_1	~1%	Zhang et al. 2018 [16] (Based on 50 images)
BEC_2	~2%	This study (Based on 50 images)
BEC_3	~3%	This study (Based on 50 images)
Conventional reactor control	~25 %	This study (Based on 50 images)
Conventional reactor (Inverse fluidized bed reactor)	~99 %	Negi et al. (2020) [28]
Conventional reactor (Up flow anaerobic sludge blanket reactor)	~38 %	Wadgaonkar et al. (2018) [29]
Conventional reactor (Packed bed reactor)	~99 %	Viamajala et al. (2006) [30]
Conventional reactor (Inverse fluidized bed reactor)	~10 %	Sinharoy et al. (2019) [31]
Conventional reactor (Membrane biofilm reactor)	~20 %	Ontiveros-Valencia et al. (2016) [32]
Conventional reactor (Continuous stirred tank reactor)	~10 %	Jain et al. (2016) [33]

662 Note: The percentage of cells having intracellular nanoparticles in conventional reactors in most of the
663 previous studies is calculated based on their limited number of TEM images.
664 Cells with intracellular Se^0 nanoparticles (%) = (number of cells containing dense and spherical
665 Se^0 particles/ total number of cells) × 100

Table 3. Mechanisms on extracellular versus intracellular Se^0 nanoparticles production on biocathode

	Extracellular Se^0 nanoparticles production	**Intracellular Se^0 nanoparticles production**
Schematics	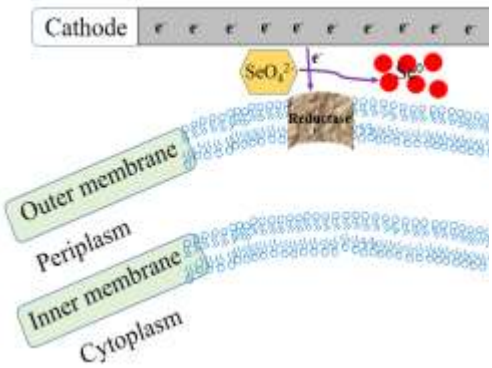	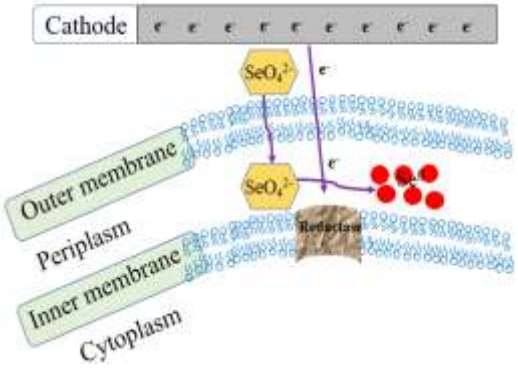
e-	Cellular energy cost for transporting electrons from biocathode to reductase: **Less**	Cellular energy cost for transporting electrons from biocathode to reductase: **More**
SeO_4^{2-}	Cellular energy cost for transporting selenate to reductase: **Less**	Cellular energy cost for transporting selenate to reductase: **More**